Journal of Applied Electrochemistry (2026) 56:112
https://doi.org/10.1007/s10800-026-02492-5

RESEARCH ARTICLE

Evaluating high-boiling binary carbonate mixtures for enhanced lithium-ion battery safety

Andreas Hofmann[1] · **Zhengqi Wang**[1,2] · **Thomas Hanemann**[1,2]

Received: 9 October 2025 / Accepted: 29 March 2026

Abstract

This study outlines how an optimized electrolyte selection can be made from a matrix of organic carbonates (dipropyl carbonate, ethylene carbonate, propylene carbonate, dibenzyl carbonate, diphenyl carbonate, 1,2-butylene carbonate, fluoroethylene carbonate) and selected conductive salts ($LiBF_4$, lithium bis (trifluoromethanesulfonyl)imide, lithium bis(oxalato)borate, lithium difluoro oxalatoborate). An optimized electrolyte design was thus achieved with a focus on electrolyte safety and electrolyte performance. For this purpose, physicochemical methods (solubility, phase transitions, density measurement, conductivity measurement, viscosity measurement) and electrochemical methods (cyclic voltammetry, corrosion tests, lithium mobility, cell tests) are presented, which were used to select the electrolyte in a reasonable and meaningful way. Finally, three electrolyte systems were identified and evaluated against a standard reference electrolyte (ethylene carbonate/dimethyl carbonate + $LiPF_6$). It was found that the electrolytes exhibit comparable performance at low to medium currents and have a significantly improved flash point. However, the self-ignition temperature is in a similar range to that of the standard electrolyte. The novel electrolyte formulations can thus help to improve cell safety by delaying the flammability of the electrolyte in the event of a spark. In addition, automatic electrolyte optimization, which is becoming increasingly important today, can benefit from the selection process, which shows how individual measurements will influence the selection.

Graphical Abstract

Electrolyte screening and selection for improved battery electrolyte safety

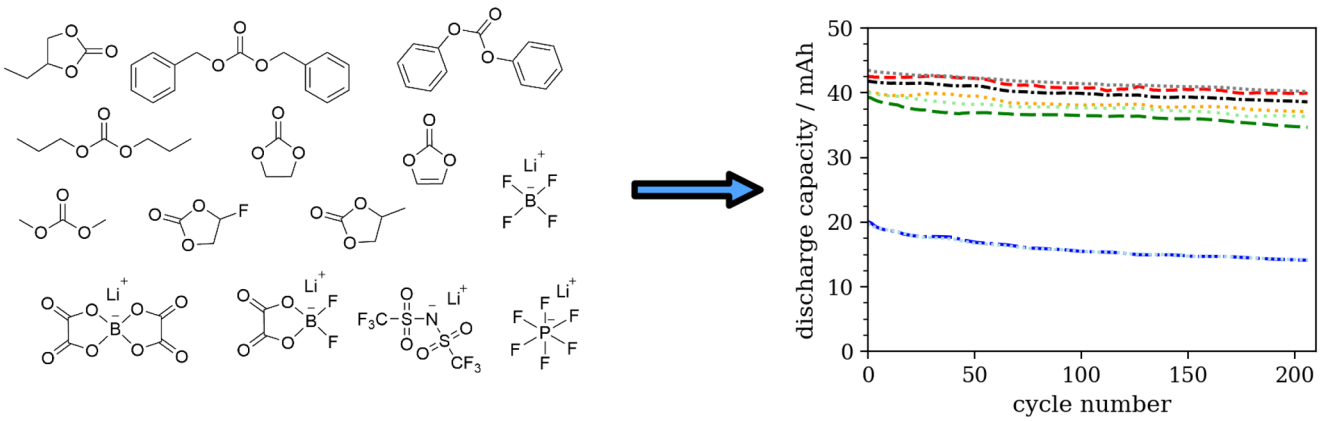

Keywords Lithium-ion electrolyte screening · Electrolyte safety · Organic carbonate solvents · Electrolyte flammability

✉ Andreas Hofmann
andreas.hofmann2@kit.edu

[1] Institute for Applied Materials (IAM), Karlsruhe Institute of Technology (KIT), Hermann-von-Helmholtz-Platz 1, 76344 Eggenstein-Leopoldshafen, Germany

[2] Department of Microsystems Engineering, IMTEK, University of Freiburg, Georges-Köhler-Allee 102, 79110 Freiburg, Germany

Published online: 03 May 2026

1 Introduction

Electrolytes with improved safety are still a major research focus today, despite all the advances made in Li-ion cells. This is a result of the need to improve battery safety not only through external features (e.g., battery management system, BMS), but also by optimizing intrinsic cell characteristics. Options for improving flammability on electrolyte level include the use of solid or gel electrolytes [1–4], the use of electrolyte additives [5–7], or the use of intrinsically flame-retardant liquid electrolytes [8, 9] including deep eutectic electrolytes [10, 11] and ionic liquids [12–15]. Phosphates, for example, are often proposed as additives or solvent components to effectively suppress the initiation of combustions [7, 16]. Furthermore, fluorinated compounds are known for their excellent safety properties [17], but have the disadvantage of potentially being classified as per- and polyfluoroalkyl substances (PFAS) compounds [18, 19]. Notwithstanding, the solvent mixture used also largely determines the hazard associated with flammability in terms of its chemical characteristics.

Another research field currently undergoing intensive research is the automatic improvement of electrolyte formulations [20], e.g., with regard to ion mobility or rate performance. In order to narrow down the large matrix of combinations, electrolyte key-properties such as conductivity and stability measurements are already being carried out automatically [21]. Nevertheless, screening requires a selection of possible substances, which are then examined in the further process, so that despite all automation, initial parameters still have to be specified. In this context, the question often arises as to which measurements are reliably suitable for carrying out material selection processes. It must always be kept in mind that additives are a very powerful tool for using electrolytes that would otherwise not function, e.g., in the case of corrosion or inadequate graphite intercalation [22–25]. Therefore, preselection processes must always focus on which properties can be relatively easily changed by additives in such a way that use in a battery becomes possible, in order to avoid omitting any promising electrolytes.

Due to their balanced properties, carbonate mixtures are still widely used today as electrolyte solvents. Typical carbonates and their electrochemical properties are summarized in Table 1. Organic carbonates were selected for this purpose due to their higher boiling temperature and the resulting higher flash points, meaning that short-chain linear carbonates (dimethyl carbonate, diethyl carbonate, etc.) are not included [26]. On the other hand, the viscosity values indicate that the higher-boiling carbonates have the potential to provide the required degree of ion mobility. As can be seen from the table, the flash point of a typical common mixture (EC/DMC/$LiPF_6$) is significantly lower than that of the higher-boiling carbonates.

Furthermore, Table 2 lists typical conductive salts that are commonly used as lithium sources, along with their key advantages and disadvantages [17]. Despite its balanced properties, $LiPF_6$ as a conductive salt is sensitive to hydrolysis with the tendency to form fluorine-containing toxic products (HF, PF_3, $OP(OH)_xF_y$) [27], etc., so this salt was only considered as a reference salt in the study. On the other hand, there are salts available that are very stable to hydrolysis and release HF to a significantly lesser extent. The extent to which HF formation enables the development of a stable solid electrolyte interface (SEI) layer illustrates the complex interplay between electrolyte and battery cell, which obviously makes selection challenging. Nevertheless, additives are commercially available nowadays that enable a LiF-rich SEI [28–31].

The aim of the study is to investigate the extent to which screening is possible in order to obtain electrolyte formulations with improved electrolyte safety, and which parameters are most meaningful in such screening with regard to material selection. The aim was to identify a mixture for each conductive salt that has promising properties in terms of battery life and exhibits superior safety characteristics compared to state-of-the-art carbonate-based electrolytes.

Table 1 Overview about characteristics of all solvents used in the study

Solvent	abbr	CAS	Density at 25 °C/g cm^{-3}	Viscosity at 25 °C/mPa s	T_m/°C	T_{bp}/°C	T_{fp}/°C
1,2-Butylene carbonate	12BC	4437-85-8	1.147	3.2	− 45	281	135
Dibenzyl carbonate	DBC	3459-92-5	1.133[a]	13.2[a]	29–33	180–190[b]	113
Diphenyl carbonate	DPC	102-09-0	–	–	79–82	301–302	167–168
Dipropyl carbonate	DPrC	623-96-1	0.944	1.1[a]	− 41[a]	167–168	55
Ethylene carbonate	EC	96-49-1	1.321	2.6	35–38	244–245	143
Fluoroethylene carbonate	FEC	114435-02-8	1.504	4.1	18–23	210	> 102
Propylene carbonate	PC	108-32-7	1.355	2.5	− 55	240–243	132
EC/DMC/$LiPF_6$	LP30	–	1.296	4.4	− 20	90	25

Standard uncertainties are $u(\rho) = 0.01$ kg m^{-3}, $u(T_m) = 2$ K, and $u(p) = 1$ kPa

T_m melting point, T_{bp} boiling point, T_{fp} flash point, *abbr.* abbreviation in the manuscript

[a]Data are taken from own measurements. Otherwise, data are taken from the supplier

[b]At pressure of 2 mm Hg

Table 2 Characteristics of the conducting salts used in the study

Solvent	CAS	T_m/°C	T_{dec}/°C	Main characteristics
$LiBF_4$	14283-07-9	293–300	162	B–F bond less labile than P–F bond, better cell performance at low temperatures, moderate ionic conductivity, high electrochemical oxidation stability
LiTFSI	90076-65-6	234–238	340	Good thermal stability, high ion dissociation, high electrochemical oxidation stability, strong resistance to hydrolysis, anodic dissolution on the Al substrate
LiDFOB	409071-16-5	265–271	200	Higher solubility than LiBOB, better SEI formation on graphite than $LiBF_4$, good cell performance at high temperatures, low interfacial impedance, cathode passivation
LiBOB	244761-29-3	>300	293	Limited solubility, stabilization of the SEI layer on the anode and protection of graphite against solvent co-intercalation and exfoliation, thermally stable SEI film, cathode passivation, hydrolysis-sensitive but more stable than $LiPF_6$
$LiPF_6$	21324-40-3	200	91	High ionic conductivity and mobility, high electrochemical oxidation stability, passivation of the Al substrate. The P-F bond is labile to hydrolysis and exhibits thermal instability

Data are taken from the supplier

T_m melting point, T_{dec} temperature of decomposition

2 Experimental

2.1 Chemicals and materials

All electrolytes were prepared in an argon-filled glove box (MBraun GmbH) with an oxygen and water level below 0.5 ppm. The materials used, such as conductive salts, solvents, additives including purity are listed in the supporting information (Table SI-5). Prior to preparation, the liquid substances were dried using molecular sieve (3 Å)and filtered through a syringe filter (0.45 µm). The conductive salts were dried in a vacuum oven at 120 °C for 5 days. The electrolyte LP30 (1 M $LiPF_6$ in a solution of EC:DMC, 1:1 Vol.%) was used as a reference sample.

2.2 Conductivity

The conductivity of the liquid electrolyte mixtures was measured using a measuring cell (0.85 mL sample volume, closed cell, RHD instruments) in the temperature range from 0 to 80 °C. Prior to the measurement, the samples were thermally equilibrated for 30 min in a humidity-controlled, temperature-controlled chamber (SH-261, ThermoTec Espec). The measurement was performed using the standard complex impedance method (Zahner Zennium IM6) using a frequency range from 1 kHz to 1 MHz, an amplitude of the applied voltage of 10 mV (measurement uncertainty $u(C) = 0.01$ C). At the phase minimum, the impedance value $|\vec{Z}|$ was related to the cell constant C and the specific conductivity κ using the relationship $\kappa = C/|\vec{Z}|$. The cell constant C is related to the geometric factor of the measurement sample and was obtained by measuring a standard solution of 0.01 M KCl solution ($\kappa = 1.413$ mS cm^{-1} at 25 °C).

2.3 Viscosity

The dynamic viscosity was measured using a rotational rheometer (Malvern Gemini HR Nano, Worcestershire, UK) in the range of $T = 15$–80 °C (shear rate of 100 s^{-1}). The electrolyte samples were placed between a 30 µm gap between a cone (with a geometry of 40/1°) and the stainless-steel plate. These experiments were carried out using a protective cover to prevent solvent evaporation into the air.

2.4 Density

The temperature-dependent density values were determined by measuring the electrolyte mixture (approx. 1 mL) between 20 and 80 °C using the DMA 4500 M device from Anton Paar (standard uncertainty $u(T) = 0.01$ °C).

2.5 DSC measurement

The phase transition temperatures were measured using differential scanning calorimetry (DSC) with the DSC 204 F1 Phoenix® calorimeter (Netzsch). The electrolyte samples were sealed in aluminum pans under an Ar atmosphere (in a glove box) in quantities of 10–15 mg. The measurement was carried out in the application temperature range from − 120 °C to + 120 °C with a heating/cooling rate of 10 K min^{-1} (standard uncertainty $u(T) = 3$ K).

2.6 Cyclic voltammetry and Al corrosion

Cyclic voltammetry (CV) was performed on a Zahner XPOT potentiostat (Zahner-Schiller GmbH & Co. KG, Kronach, Germany). The cells from EL-Cell GmbH were measured in a 2-electrode configuration with Li (Ø = 15 mm, reference electrode), platinum (Ø = 18 mm, working electrode) and a glass fibre membrane (GF/B, Ø = 18 mm) including the electrolyte (volume: 160 µL) in between. The potential range for anodic scanning was set at the working electrode

Pt at a speed of ± 1 mV s^{-1} from 3.0 to 6.5 V vs. Li^+/Li. The investigation of anodic aluminum dissolution was carried out in a two-electrode configuration (Swagelok® cell) with aluminum foil (Ø = 12 mm) as the working electrode, lithium foil (Ø = 12 mm) as the reference electrode and a glass fiber separator (GF/A, Ø = 13 mm; electrolyte volume: 40 µL) between them. The cells were assembled in a glove box and operated in the range of 2.5–4.3 V with a rate of 1 mV s^{-1} at 23–25 °C. The Al foils obtained from the disassembled cells after the cycle were cleaned with DMC, acetone and isopropanol to remove electrolytes and traces of conductive salt and observed under a microscope (AX70, Olympus).

2.7 Lithium mobility

Lithium ion mobility was measured using programmed chronopotentiometry in Swagelok cells with two electrodes at the Zahner Zennium IM6 electrochemical workstation. Lithium metal (foil, Alfa Aesar, Ø = 12 mm) is used as the working, reference and counter electrode in the cell, with a glass fiber separator (Whatman, GF-B, Ø = 13 mm) placed between the two electrodes. It was observed that almost identical I_{max} values were found regardless of whether 4 or 6 layers of glass fiber separators were used in the cell (33.5 ± 0.2 mA, test electrolyte: EC/EMC + 1 M $LiPF_6$). Two layers result in slightly reduced values, so 4 layers are used for the investigation. 75 µL of electrolyte solution is used for each separator layer. The cells were pre-polarised at $\beta = 1$ mA s^{-1} from OCV to 0.7 V and then measured (after relaxation of the potential) at $\beta = 20$ µA s^{-1} to 10 V.

2.8 Battery cells

All cell components for the battery tests were dried in a vacuum oven at 95 °C for 24 h before cell assembling. Battery tests in the form of button cells were performed using a cell cycler (Astrol, Othmarsingen, Switzerland). The potentials specified in this work are those of the cathode electrode relative to the counter electrode. The charging and discharging cycles were performed at current rates (C-rate) based on the capacity of the NMC cathode material (NMC-111, Custom cells, Itzehoe, Germany) used. In cell tests, CR-2032 coin cells (SUS 316L from Hohsen Corp.) were assembled using a hydraulic crimper MSK-110 (MTI Corp.). For half-cell tests, a lithium foil (Alfa Aesar, Ø = 15 mm), a NMC cathode (2 mA cm^{-2} Ø = 16 mm) and a glass fiber separator (Whatman, GF/B, Ø = 16 mm) with an electrolyte volume of 130 µL were used with a spring and a stainless-steel spacer (0.5 mm) and carried out between 3 and 4.3 V. Instead, a NMC cathode (2 mAh cm^{-2} with a deviation of ± 5%, Ø = 16 mm), a graphite anode (Custom cells, Itzehoe, Germany, 2.2 mAh cm^{-2} with a deviation of ± 5%, Ø = 16 mm) and a glass fiber separator (GF/B, Ø = 16 mm; electrolyte volume: 130 µL) with a spring and stainless steel spacers are used for full cell coin cells and carried out in the voltage range 3–4.2 V. The pouch bag cell was assembled with graphite (anode), NMC (cathode) and separator (Separion, impregnated with 450 µL electrolyte) and constructed in a dry room. The pouch bag cells were cycled in an 8-channel battery test system BST-5V3A using BTSDA software, the test data analyser from Neware Technology. The formation protocol of the cell cycling was determined by 7 cycles at different C-rates (1 cycle with 0.05 C charge and 0.07 C discharge, 5 cycles at 0.2 and 0.23 C, and 1 cycle at 0.1 and 0.1 C, based on a capacity of 44 mAh cathode NMC) in the voltage range 3.0–4.2 V. The battery tests were controlled at 25 °C.

2.9 Flash point and auto ignition temperature

The flash points were measured using a flash point determination device (Anton Paar Miniflash FLP Touch, 0–200 ± 0.1 °C, Grabner Instruments) in accordance with ASTM D6450. The electrolyte sample was taken in the sample holder and heated at a heating rate of 5.5 °C min^{-1} until the lowest temperature was measured at which an ignition source ignited the vapor phase of a sample. The measurement was pre-calibrated with the certified reference material (decahydronaphthalene). Auto ignition temperature was measured from Analytische Laboratorien (51789 Lindlar, Germany).

3 Results and discussion

3.1 Selection of solvents and conducting salts including salt solubility

The aim of the study is to identify novel electrolyte formulations with superior safety characteristics based on carbonate solvents. In order to realize this objective, a matrix of seven carbonates and four conductive salts was selected and examined in detail. The selection was based on considerations to remain in a carbonate system, to achieve increased electrolyte safety as a result of delayed flammability, to select commercially readily available solvents and conducting salts, and to keep the fluorine content in the solvents as low as possible. The chemical structures of the compounds used are shown in Fig. 1. Figure 2 shows the individual analysis tools used to conduct the selection process, whereby one step may involve several analyses. In the final step of the evaluation (testing in battery cells), additives were used to suppress adverse effects of the electrolytes

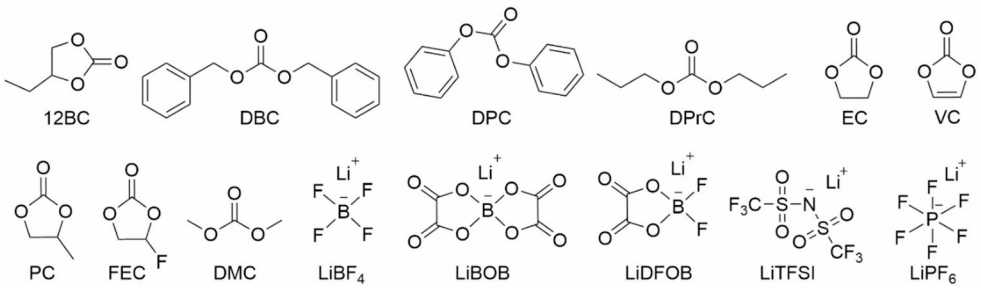

Fig. 1 Chemical structures of all solvents and salts used in the study

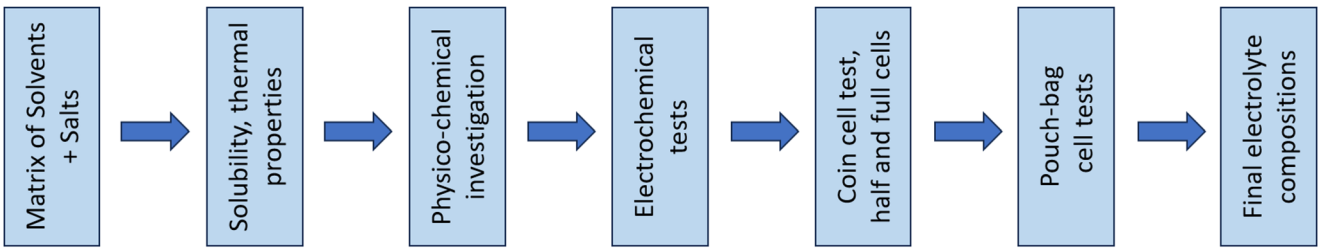

Fig. 2 Flowchart of the analyses performed

Table 3 Evaluation of phase characteristics and miscibility of binary mixtures of organic carbonates and conducting salts

Conducting salt and solvent mixture[a]		Solubility of 0.75 M conducting salt					T_m/°C < − 20 °C[b]				
Conducting salt	sol-2 / sol-1	FEC	DPrC	DBC	12BC	PC	FEC	DPrC	DBC	12BC	PC
LiTFSI	EC							4			
$LiBF_4$							–	–	–		**− 88**
LiDFOB							–	**− 54**	–		
LiTFSI	PC					–		**− 91**			–
$LiBF_4$						–	–	**− 58**	19	**− 93**	–
LiDFOB						–	–	**− 59**	–		–
LiTFSI	12BC				–	–				–	–
$LiBF_4$					–	–	–	**− 62**	16	–	–
LiDFOB					–	–	–		18.8	–	–
LiTFSI	DBC			–	–	–		15	–	–	–
$LiBF_4$				–	–	–	–	–	–	–	–
LiDFOB				–	–	–	–	–	–	–	–
LiTFSI	DPrC		–	–	–	–		–	–	–	–
$LiBF_4$			–	–	–	–	–	–	–	–	–
LiDFOB			–	–	–	–	–	–	–	–	–

Insoluble mixtures (i.e. the salt did not dissolve completely in a 0.75 M concentration) and mixtures with a melting peak above − 20 °C are marked in color red. Fully homogeneous miscible systems and mixtures with a melting point below − 20 °C are marked in green. Only the mixtures that tested positive for solubility were examined for melting point

[a] *Sol* solvent

[b] If a melting point above − 100 °C could be detected (DSC), this is indicated as a number

(e.g. Al corrosion), which occur in particular when using TFSI-containing conductive salts. Generally, it should be noted that the limits for individual measurements should not be set too low, so as not to reject electrolytes solely on the basis of a single poor value, even though the mixture as a whole might still have balanced characteristics.

Initially, it was examined whether the solvents could be completely blended at room temperature and whether at least 0.75 mol/kg of conductive salt was soluble in the mixture. This amount corresponds to a concentration of approximately 1 M. In addition, it was verified whether the mixtures had a melting point below − 20 °C, enabling their use under normal conditions. Since none of the mixtures with DPC or LiBOB resulted in homogeneous solvent/conductive salt combinations, DPC as well as LiBOB were not included in the table and immediately discarded. The remaining compounds are shown in Table 3, with immiscible or higher-melting mixtures marked in red.

Mixtures containing LiTFSI in particular exhibit good solubility and low melting points. Based on miscibility/solubility and melting point characteristics, 24 potential mixtures were selected for further investigation. From the originally possible 84 electrolytes (21 solvent combinations

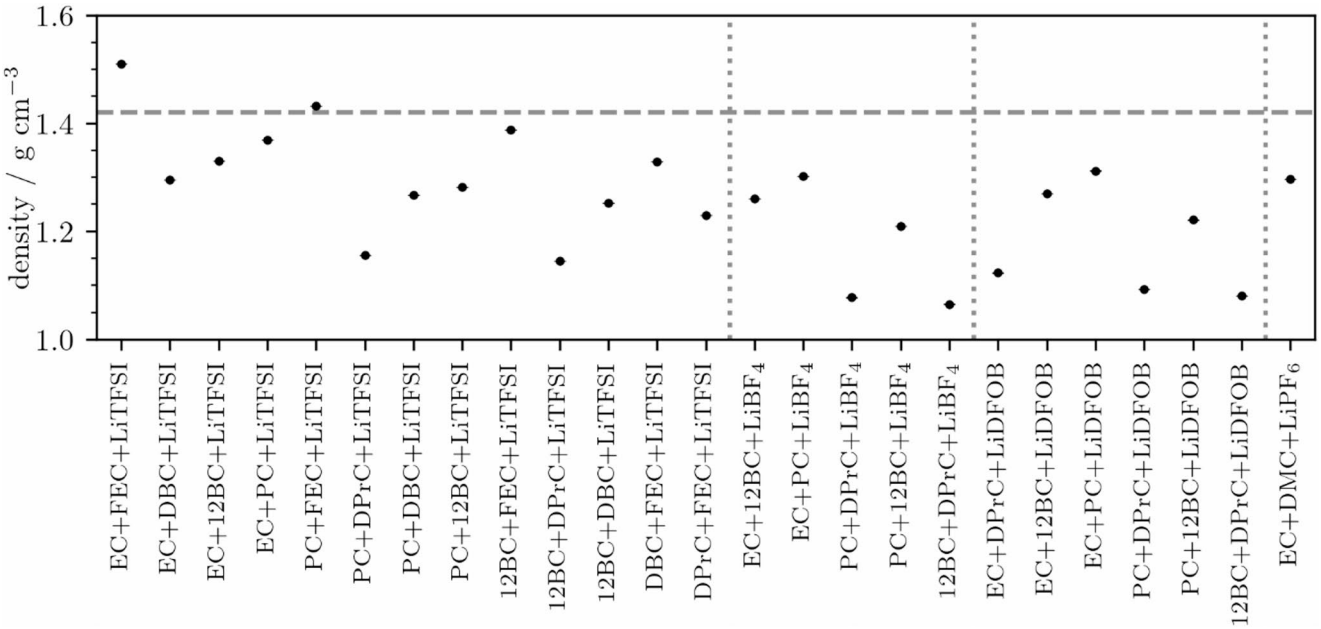

Fig. 3 Density values at $T = 25$ °C for all mixtures that received a positive rating in Table 3

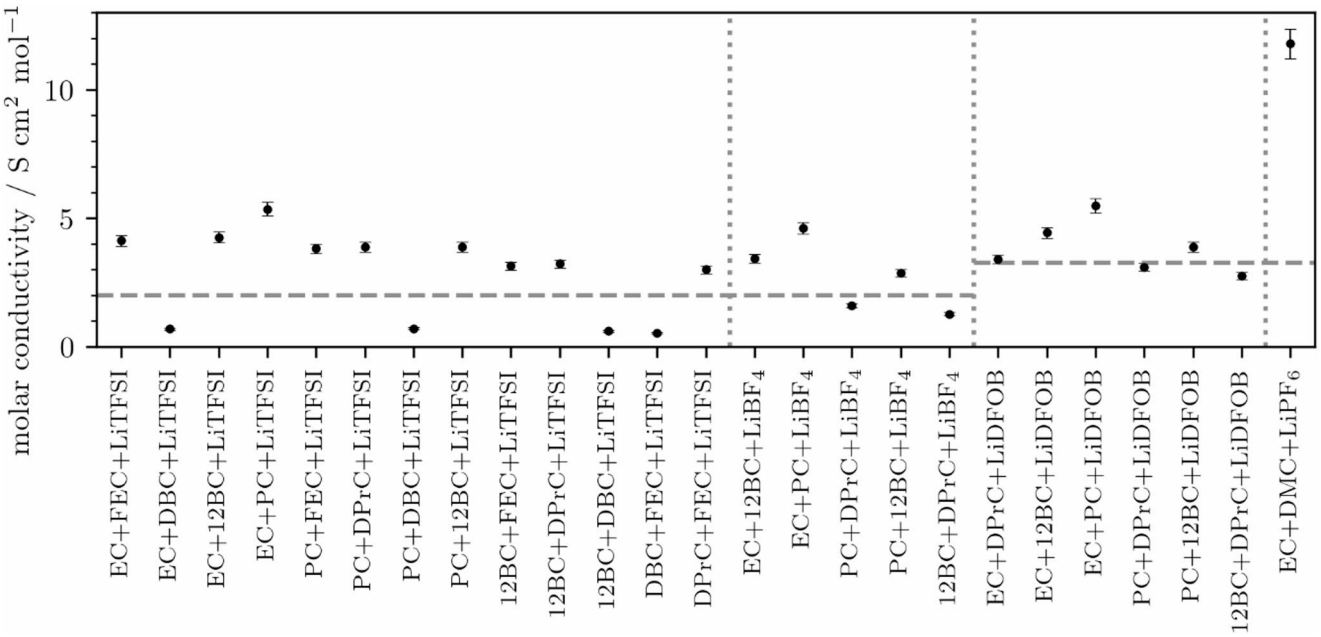

Fig. 4 Molar conductivity values at $T = 25$ °C for all mixtures that received a positive rating in Table 3

and 4 conductive salts), 60 combinations could be excluded in the first step, considerably reducing the matrix.

3.2 Physicochemical properties: density, conductivity, viscosity

In order to further evaluate the suitability of the electrolytes for their use in batteries, easy-to-perform physical–chemical measures were carried out. The values at 25 °C for density (Fig. 3), molar conductivity (Fig. 4) and dynamic viscosity (Fig. 5) are shown below. The following lists all mixtures with a salt concentration of 0.75 mol kg^{-1} and a 1:1 weight ratio of the solvents.

Since high density values of the electrolytes significantly reduce the energy density of the battery, a maximum value of 1.42 g cm^{-3} was tolerated here. This value corresponds to the density value of the standard electrolyte with an additional 10%. High viscosity or low conductivity contributes

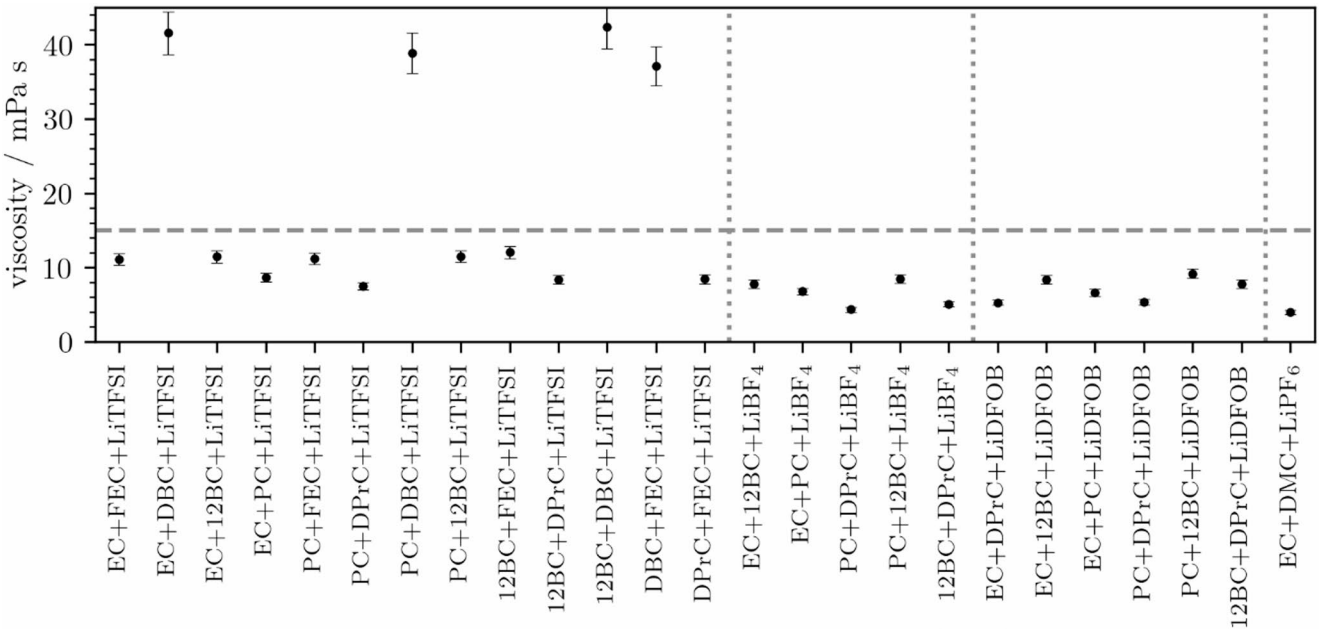

Fig. 5 Dynamic viscosity values at $T = 25$ °C for all mixtures that received a positive rating in Table 3 at shear rate of 100 s^{-1}

to high internal resistance and poor ion mobility in a battery cell. For this reason, a viscosity above 15 mPa s and a molar conductivity below 2 S cm^2 mol^{-1} were also set as exclusion criteria. Since the conductivity values are generally higher in the case of LiDFOB mixtures, a limit of 3.25 S cm^2 mol^{-1} was defined in this case. The limits were chosen to avoid accidentally ruling out promising electrolytes too early on by setting overly rigid limits. All limit values are marked as horizontal lines in the figures. It should be noted here that the molar conductivity of all mixtures examined is approximately three times lower than that of a commonly used standard electrolyte system currently in use. However, the high conductivity of the reference electrolyte is achieved at the expense of a very low flash point. An example of a corresponding density, viscosity and conductivity measurement is shown in the supporting information (Figs. SI-1–SI-4) for the mixture FEC + 12BC + LiTFSI.

The temperature dependence of conductivity and viscosity (see Fig. SI-5, supporting information) did not result in any significant additional restrictions, so it can be noted here that, based on this screening to narrow down suitable combinations, a temperature-dependent, time-consuming measurement would not have been necessary in this case. Temperature-dependent values are, of course, essential in order to be able to provide a final assessment, but this can also be done at the end with the final electrolyte formulations. This significantly reduces the amount of measurement work required. In summary, a total of 10 mixtures were discarded due to their unfavorable properties, mainly for reasons of conductivity, based on the density, conductivity, and viscosity measurements performed. The remaining 14 mixtures were examined further using electrochemical methods.

3.3 Electrochemical properties: Li mobility, cyclovoltammetry, Al corrosion

The influence of the applied electrical voltage on the rate-dependent ion movements in an electrolyte mixture or on the kinetic limit of ion movement can be studied using chronopotentiometry (Fig. 6) [32]. During the measurement, an increased current is applied between the symmetrical Li electrodes of the measuring cell so that an increasing potential is generated. At the start of the measurement , the electrolyte components between the two Li electrodes are polarised. With increasing applied current, a higher lithium-ion flux is enforced, which in turn leads to an increase in the measured cell voltage. With faster lithium deposition, the concentration gradient of lithium ions near the Li electrode surface changes dynamically. The more ‘efficiently’ the oxidized ions are brought close to the electrode by ion diffusion, the more ions per unit of time could participate in the redox reaction at the same voltage, or the lower the voltage applied to the electrode at a given current density. Therefore, the slope of the U/I curve in the linear initial range can be considered as a measure of the difficulty of ion movement. LP30 shows the lowest slope of $\Delta U/\Delta I$. This means that a slower voltage increase $U(t)$ is required to apply the linearly increasing current $I(t)$. For this reason, the highest ion mobility is observed for LP30, which corresponds well with the ion conductivity in the Fig. 4. In this study, a maximum gradient of 0.75 was still considered acceptable.

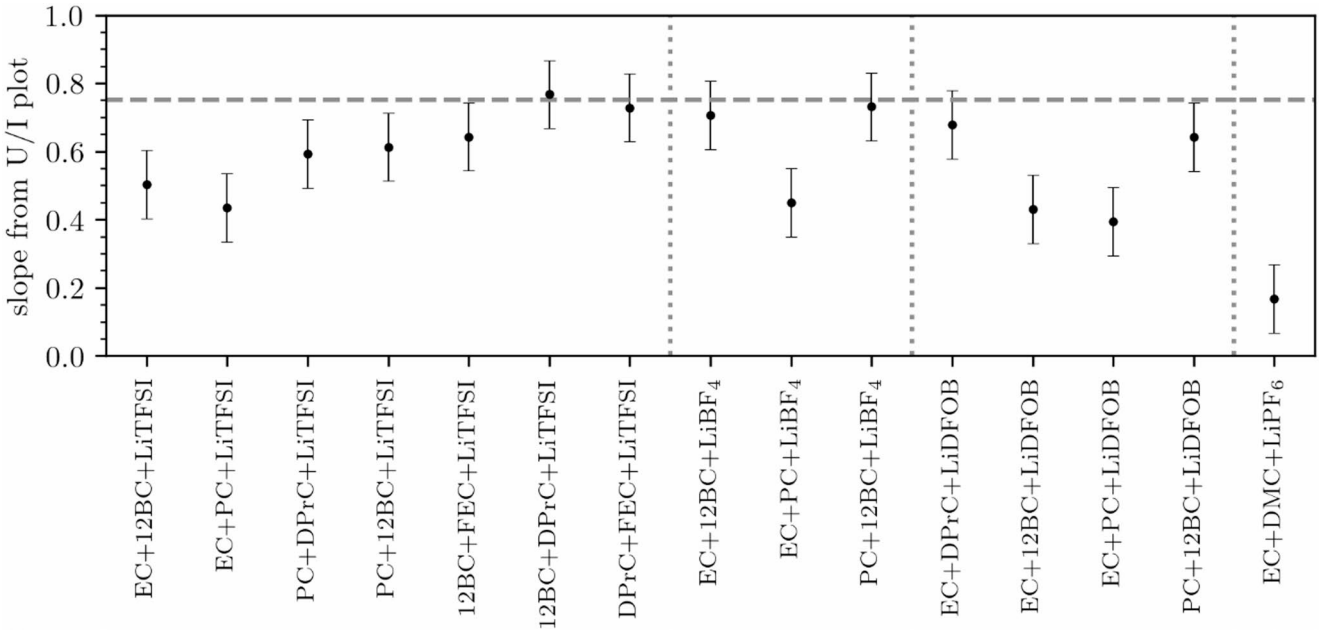

Fig. 6 Slope from *U*/*I* plots for all mixtures that received a positive rating in Sect. 3.2

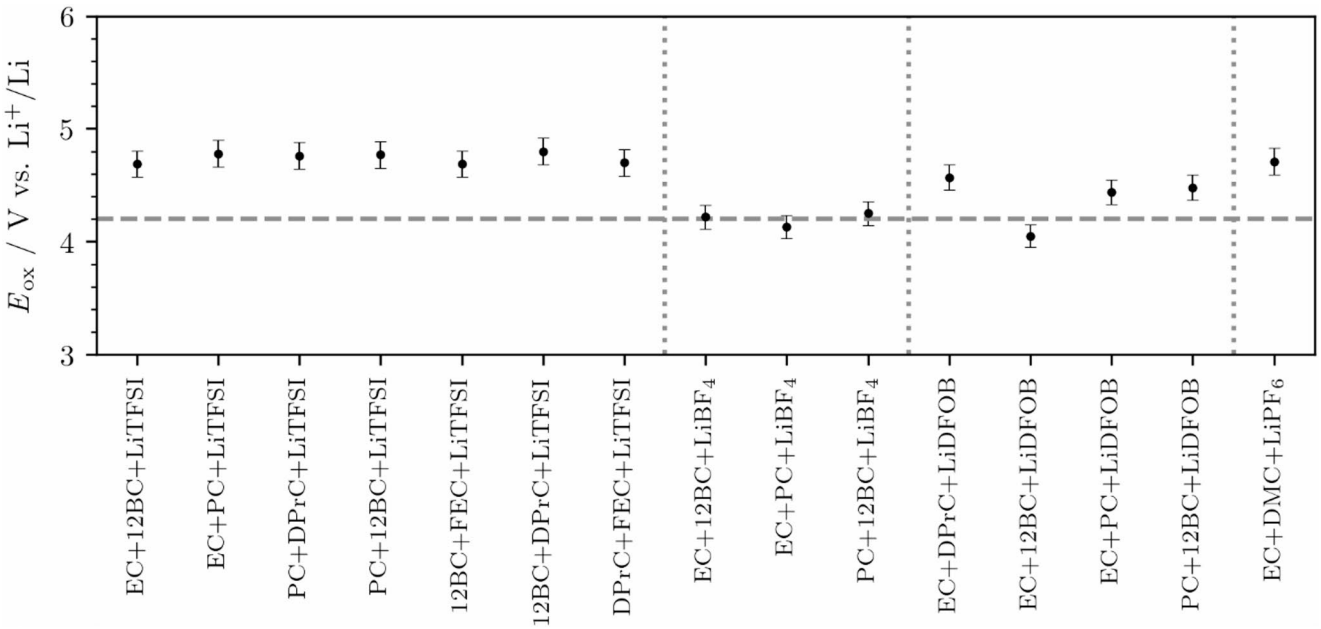

Fig. 7 Oxidative stability from Pt|Li cells for all mixtures that received a positive rating in Sect. 3.2

However, as the measurements show that all values are relatively close together, only one mixture was discarded in the end. Even though the measured variable is similar to conductivity using platinum inert electrodes, active Li ions are moved here and their behavior is examined. On the other hand, boundary layer effects due to the reactive lithium electrode used also play a role. The intention here was to examine direct Li mobility. However, it has been shown that the added value compared to pure conductivity remains limited.

The oxidation potential E_{ox} of the electrolyte mixtures was measured using cyclovoltammetry (CV, Fig. 7). The oxidation potentials shown were obtained at a nominal current density I = 30 µA (approx. 11.8 µA cm^{-2}, based on the diameter of the Pt electrode). The oxidation stability was essentially influenced synergistically by the salts or carbonates used. In Fig. 7, the reference sample LP30 has an oxidation potential of approximately 4.7 V vs. Li/Li^+. The LiTFSI-based mixtures exhibit relatively higher oxidation stability, followed by LiDFOB and LiBF4. The C-F bonds

of the TFSI anion are quite stable and less prone to oxidation [33].

Remarkably, the E_{ox} values of mixtures based on 1,2-BC + DPrC were higher than the others. The increased oxidation stability was attributed to the linear structure of DPrC and the butyl substituent in 1,2-BC. A critical stability of 4.2 V was defined as the minimum criterion, even though the actual stability when using electrode materials may differ from the values obtained using inert electrodes [34]. This is also the most important issue with the measurement itself, as it has already been proven that the electrode material has a significant influence on the stability of the electrolyte. Due to the fact that all three values of the $LiBF_4$ mixtures are in the same error range, we maintained all three mixtures for the next step. It is noteworthy that the oxidative stability of the EC+12-BC + LiDFOB mixture is lower than that of comparable formulations containing other salts. This behaviour suggests that oxidative stability is not solely determined by the individual solvent or salt components, but rather by their specific coordination environment and the intermolecular interactions within the mixture. The coordination of Li^+ with the $DFOB^-$ anion may differ significantly from that with BF_4^- or $TFSI^-$, potentially leading to altered solvent–salt interactions and modified oxidative stability.

A deeper understanding of this effect would require theoretical studies, such as DFT-based analysis of ion–solvent coordination structures, which are beyond the scope of this manuscript. Finally, one mixture was identified that did not meet this criterion (EC+12BC+LiDFOB) and was not considered for further investigation. After the two more fundamental electrochemical tests (lithium mobility and anodic stability), 12 mixtures were examined in detail with respect to their Al corrosion tendency (Fig. 8).

As expected, LiTFSI showed the most pronounced effects with regard to Al corrosion, leading to significant Al pitting. Microscopy images as examples of all Al disks are shown in the supporting information (Fig. SI-6). However, it was revealed that there was a noticeable gradation within the LiTFSI electrolytes. To limit the number of TFSI mixtures, 2 out of the total of 6 mixtures were selected for further investigation. Therefore, the PC + 12BC and DPrC + FEC based TFSI mixtures were chosen. The PC + 12BC mixture was selected due to its slightly improved characteristics in terms of voltage stability values compared to the EC + 12BC mixture (even though it's almost within the same range of error). Compared to the reference electrolyte, the electrolytes based on $LiBF_4$ and LiDFOB showed even less corrosion, so that in this case all mixtures were pursued further. Based on the fundamental electrochemical investigations, seven mixtures were obtained, which were used to conduct battery tests.

3.4 Cell tests: half cells and full cells

The half-cell results in NMC vs. Li cells are shown in Fig. 9. Since significant Al corrosion was expected in the case of TFSI-containing conductive salts, the TFSI-containing electrolytes were also investigated with the additive LiBOB (1 wt%), as it is known that LiBOB can suppress corrosion processes [25]. To verify this assumption, additional corrosion tests were performed using LiBOB for comparison, which show that the corrosive behavior of LiTFSI can be actually suppressed significantly (Figs. SI-7 and SI-8, supporting information). The half-cell tests were carried out despite the critical metal anode, because carbonates (PC) can still be used relatively unprotected in this case. In

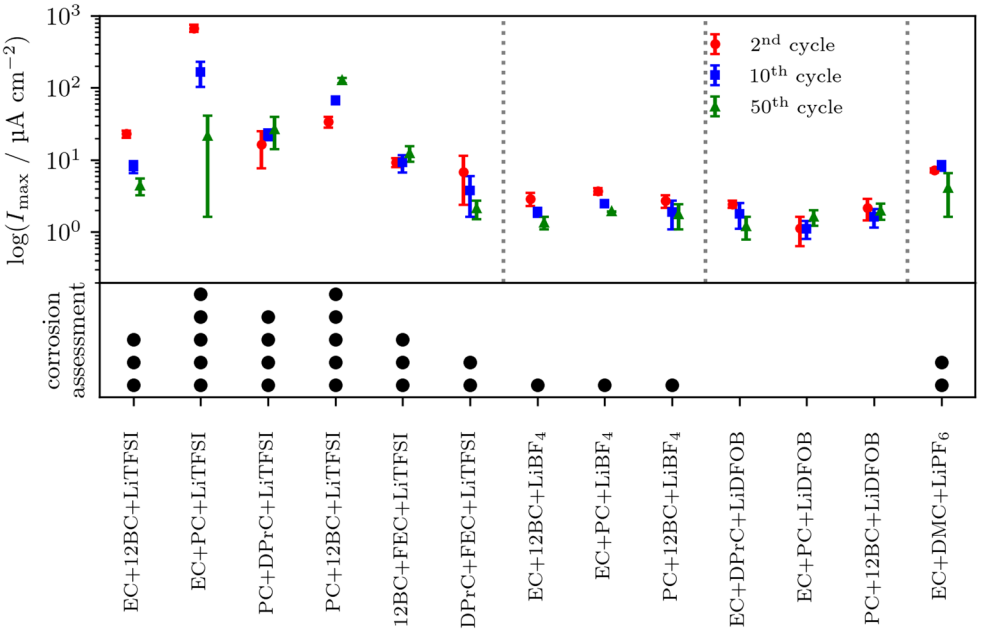

Fig. 8 Al corrosion in Al|Li cells for all mixtures that received a positive rating from Figs. 6 and 7. A qualitative assessment of the corrosion behavior is done based on microscopy of the Al foil after disabling the coin cells. The dots in the lower section indicate corrosiveness; that is, the more dots, the higher the aluminum corrosion

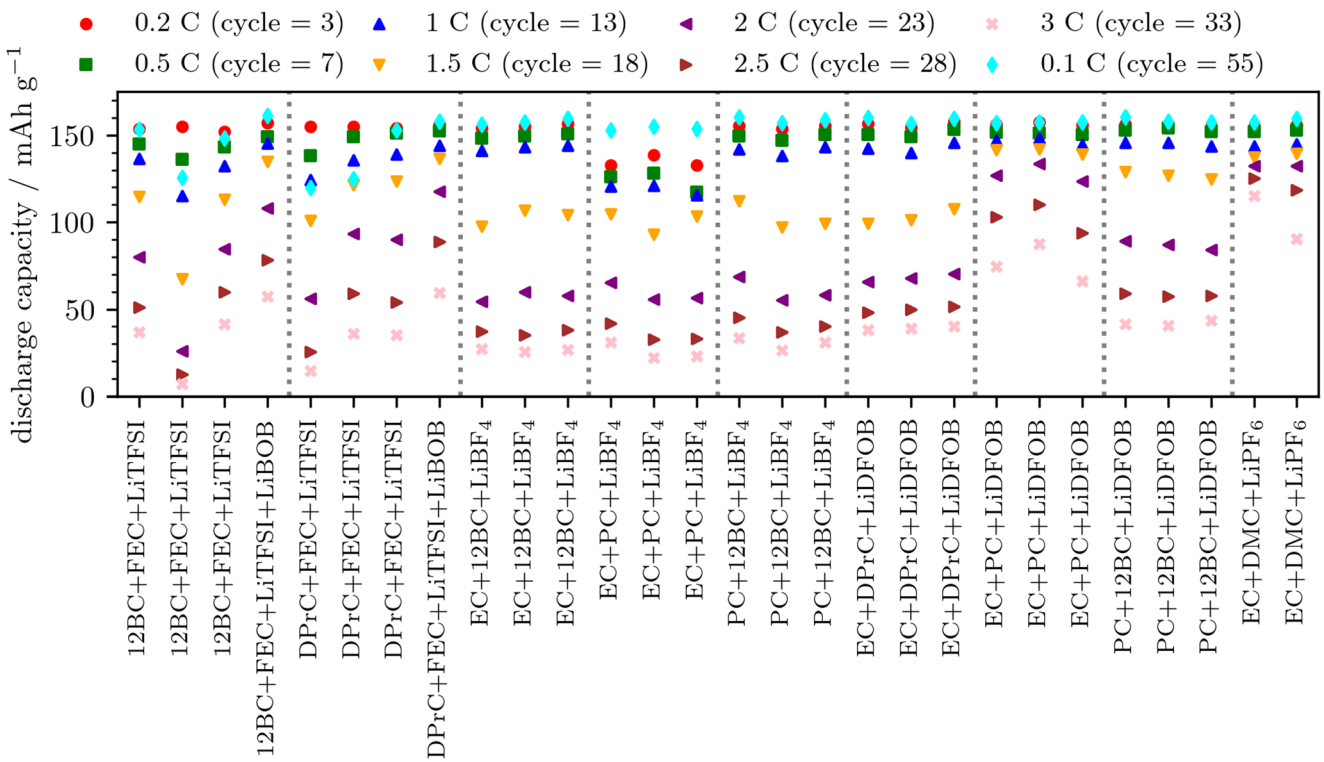

Fig. 9 NMC|Li half cell results for all mixtures that received a positive rating in Sect. 3.3. Current rates during the discharge cycle. All charging is performed at a C-rate of 0.5 C. The LiBOB concentration is 1 wt%

contrast, PC cause significant issues with graphite or require additional additives. Similar capacity values to those for the standard electrolyte were obtained at slow C-rates with the TFSI-containing mixtures including LiBOB additive. It is worth mentioning that the FEC-containing mixtures favored the formation of a LiF-rich anode interface layer (solid electrolyte interface, SEI) [35, 36]. Many studies have already shown that LiF is a common but necessary component of the SEI film on the lithium metal anode and ensures homogeneous lithium deposition and suppression of lithium dendrites [35, 36]. Reproducible acceptable values were obtained for $LiBF_4$-based mixtures, especially during slow cycling. However, capacity retention drops significantly at higher C-rates. The best results, even at faster C-rates, were obtained for the EC+PC+LiDFOB mixture. Up to almost 2C, results comparable to those obtained with the standard electrolyte were observed. The drop in capacity at higher C-rates observed at higher C-rates in the case of the reference cells can be attributed to the use of coin cells, which leads to significant deviations at higher C-rates [37].

As both TFSI-containing electrolytes exhibited similar performance, these two systems were further investigated. Since the EC+PC mixture showed the weakest performance for the $LiBF_4$ electrolyte, particularly at slower C-rates, this mixture was discarded. In the case of LiDFOB, the EC+PC-based mixture was selected, which showed significantly better performance than the other two LiDFOB mixtures.

Using these five mixtures, a series of tests were then carried out in full cells (Fig. 10). In full cell experiments the SEI becomes increasingly important with graphite anodes. In addition, it is well-known that PC and possibly also 1,2-butylene carbonate are not compatible with graphite electrodes [38]. To exclude or at least minimize these negative impacts, vinyl carbonate (VC, 1 wt%) was added to all new carbonate mixtures [39–41]. In addition, LiDFOB or LiBOB was used as a corrosion inhibitor in the case of TFSI-containing electrolytes.

Both LiTFSI-based mixtures achieve Coulomb efficiencies of up to approximately 88% in the first cycle (see Fig. 11). This has been attributed to the composition of the SEI layer. On the one hand, the FEC component can contribute to a higher LiF content. The inorganic LiF leads to a reduction in the cohesion and flexibility of the SEI layers, which limits the volume changes during the (de)lithiation of graphite [42–44]. On the other hand, the flexible TFSI anions of the salt and the lithium alkyl carbonate formed can compensate for this limitation of graphite [45]. In addition, the synergistic interaction of FEC and VC (and possibly other additives) at the two electrodes influenced the properties of the SEI layer [44, 46]. The FEC+12BC+LiTFSI-based

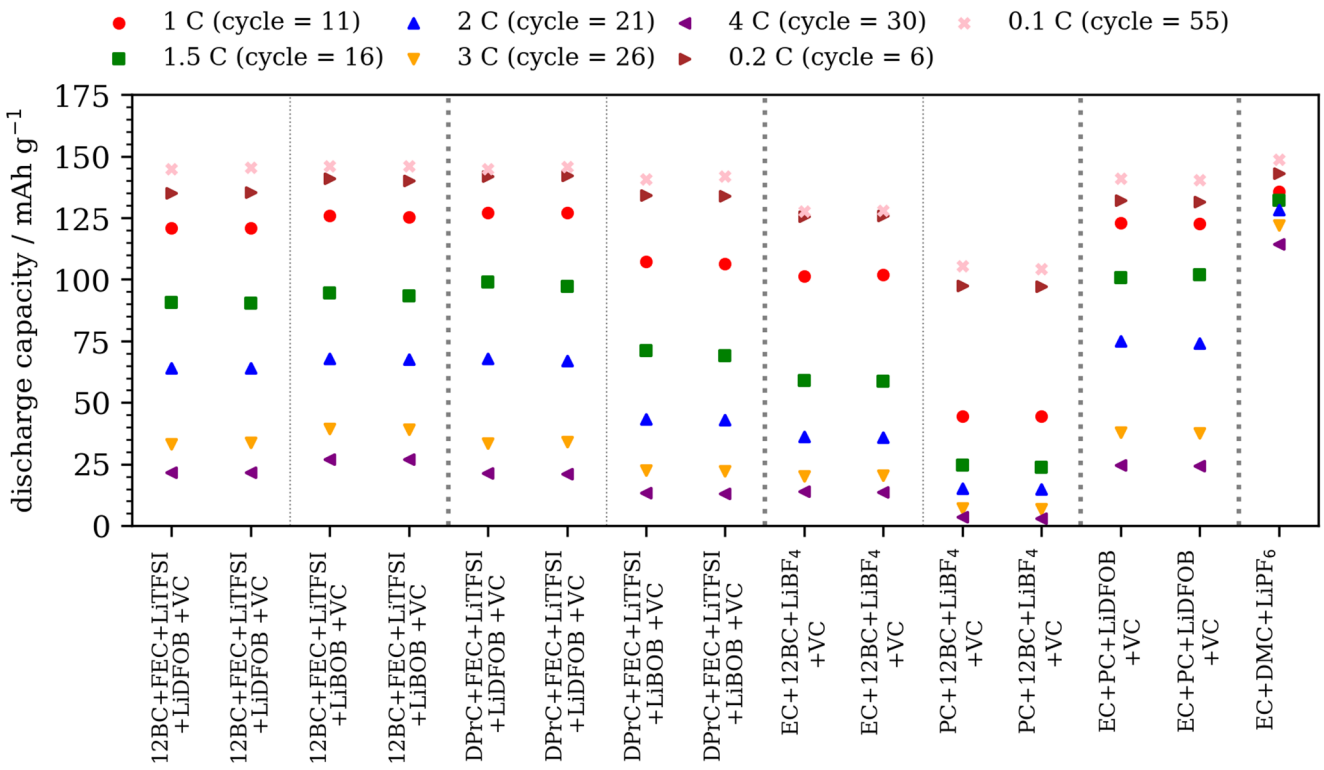

Fig. 10 NMC|graphite full coin cell results for all mixtures that received a positive rating in half cell experiments. The numbers in brackets indicate the cycle number from which the current C-rate value was taken. The concentration of additives is 1 wt% each for Li-salts and VC.

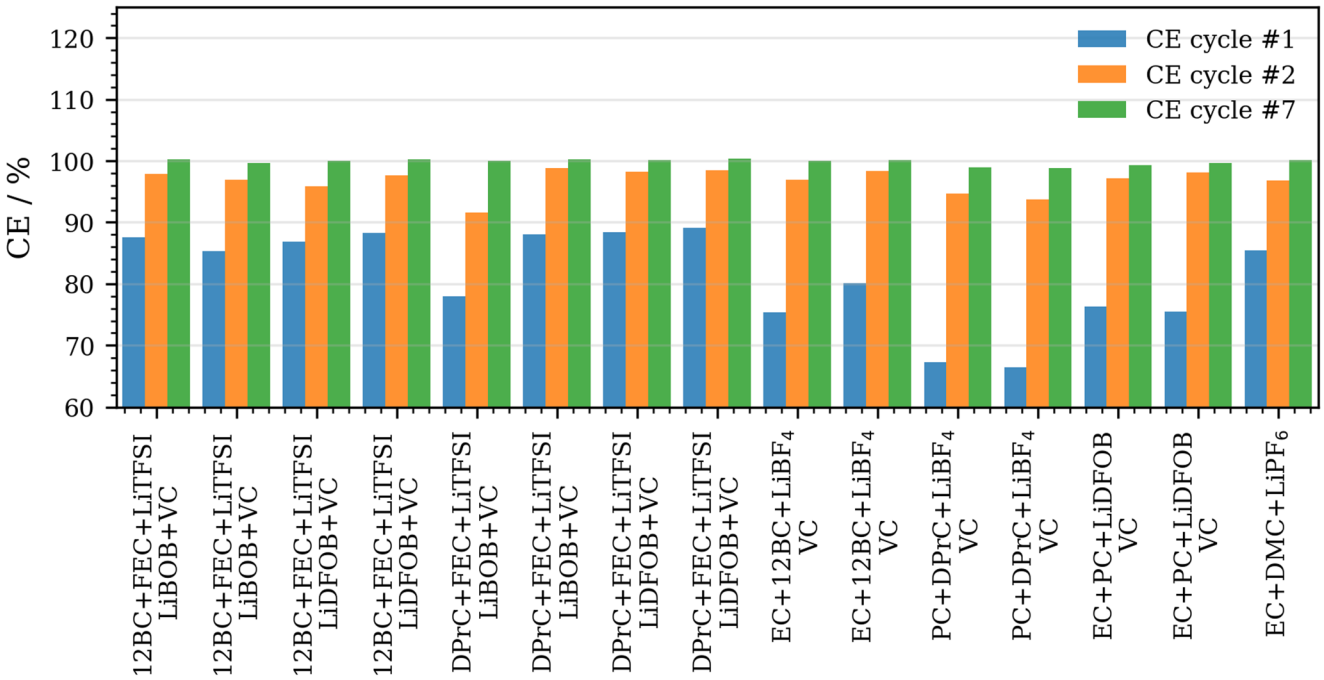

Fig. 11 Coulomb efficiency (CE) for the NMC|graphite full coin cell results for all mixtures. The concentration of additives is 1 wt% each for Li-salts and VC (same as Fig. 10).

mixture exhibits higher discharge capacity at faster discharge rates (>1 C). This is in agreement with the ion transport properties. If the cell is recharged more slowly at 0.1 or 1 C after a fast discharge protocol (up to 3 C), the FEC+12BC+LiTFSI mixture recovers nearly 100% of its original capacity. This means that in this case, only a very small amount of lithium is lost during fast charge and discharge cycles. For the $LiBF_4$-based mixture, the electrolyte with a higher EC content exhibits better C-rate performance, namely EC+12BC+$LiBF_4$. The efficiency of SEI formation by EC or PC might explain this difference, as the faster reaction occurs with EC (lower LUMO energy level) [47–49].

In accordance with the promising half-cell results for the LiDFOB electrolyte, it also demonstrated impressive performance in full-cell measurements, particularly at C-rates of up to approximately 1.5 C, where it is comparable to standard electrolytes in terms of discharge capacity. The analysis of the Coulomb efficiency (CE) (Figs. 11 and SI-9) reveals significant differences during the cell formation between the selected electrolytes. Unlike the LiTFSI and $LiPF_6$ electrolytes, the $LiBF_4$- and LiDFOB-containing electrolytes exhibit significantly less favorable CE behavior in the first cycle. It should be noted here that a high-quality measuring device must be used for the CE analysis, as current accuracy and the timely detection of charging and discharging capacitance are extremely important for this purpose. This also explains the somewhat greater variation in the values in this study (see Fig. SI-9, supporting information), as the measuring device used was only partially suitable for highly accurate measurements. In accordance to the cell tests, superior performance was also observed in the CE analysis from mixture EC+12BC+$LiBF_4$ compared to PC+DPrC+$LiBF_4$. Finally, three basic mixtures were selected, namely 12BC+FEC+LiTFSI, EC+12BC+$LiBF_4$, and EC+PC+LiDFOB. The selection was based on the consideration to include each conductive salt in at least one electrolyte mixture.

The three basic mixtures were formulated as electrolyte mixtures with the corresponding additives, resulting in three electrolyte mixtures (EL). The additives are selected based on their positive effects listed above and their well-known SEI-improving characteristics. The exact composition and their physicochemical properties are shown in Table 4.

The three selected electrolytes were evaluated in a 50 mAh pouch cell to validate the coin cell results (Fig. 12 shows two identical measurements for each case). Contrary to the positive preliminary results, the $LiBF_4$-containing electrolyte performed significantly worse than the others. It exhibited lower discharge capacity at a modest 0.2 C rate and pronounced cell aging. These deficiencies were not apparent in the preliminary tests, including button cell experiments. Importantly, the electrolytes included LiDFOB and LiBOB as a corrosion inhibitor, added to improve SEI formation and minimize negative effects on graphite anodes, consistent with the full-cell formulation described earlier. However, the observed deterioration in pouch cells is thus far more severe than expected from initial testing.

This suggests an additional effect arising from scaling up: changes in cell geometry, increased sensitivity to gas evolution and pressure, altered interactions with the separator (switching from glass fiber to polyolefin- or PET-based separators), concentration gradients, and transport limitations due to a lower electrolyte-to-electrode ratio. These factors act simultaneously, meaning that a "good electrolyte" in small cells can fail in larger formats. Furthermore, the lower oxidative sensitivity of $LiBF_4$ may contribute to sudden increases in side reactions during constant-current hold (CCCV) phases.

As the focus of this manuscript is electrolyte selection, the transition from coin to pouch cells is only briefly addressed

Table 4 Overview about the selected basic mixtures as well as the corresponding electrolyte mixtures

	FEC+12BC LiTFSI	EL-1	EC+12BC $LiBF_4$	EL-2	EC+PC LiDFOB	EL-3	LP30
Solvents (1:1 wt%)	FEC, 12BC	FEC, 12BC	EC, 12BC	EC, 12BC	EC, PC	EC, PC	EC, DMC
Conducting salt	LiTFSI	LiTFSI	$LiBF_4$	$LiBF_4$	LiDFOB	LiDFOB	$LiPF_6$
c (cond. salt)/mol kg^{-1}	0.75	0.629	0.75	0.629	0.75	0.698	1 M
Additive 1	–	VC	–	VC	–	VC	–
wt%		1		1		1	
Additive 2	–	LiBOB	–	LiBOB	–	LiBOB	–
c (add. 2)/mol kg^{-1} (wt%)		0.052 (1)		0.052 (1)		0.052 (1)	
Additive 3	–	LiDFOB	–	LiDFOB	–	–	–
c (add. 3)/mol kg^{-1} (wt%)		0.070 (1)		0.070 (1)			
ρ/g cm^{-3}	1.39	1.38	1.26	1.26	1.31	1.31	1.30
η/mPa s	12.0	11.6	7.8	7.2	6.6	6.6	3.9
Λ/S cm^2 mol^{-1}	2.7	2.5	3.0	2.8	4.8	5.1	10.6
E_{ox}/V_{Li}	4.7	4.7	4.2	4.3	4.4	4.5	4.7
Discharge capacity/mAh g^{-1} (cycle 3) (0.2 C, NMC vs. C)	–	145.5	–	144.2	–	146.0	148.1

The total Li concentration is 0.75 mol kg^{-1} for all mixtures except the reference electrolyte (1 M $LiPF_6$ in EC/DMC 1:1 Vol.%).

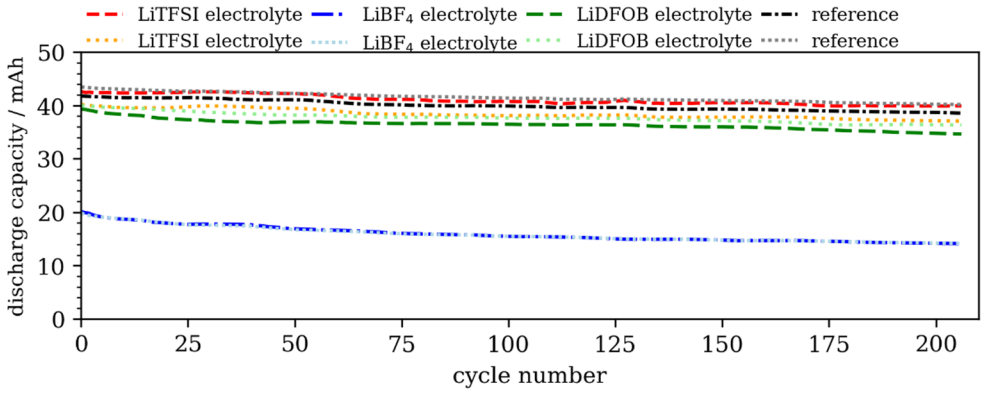

Fig. 12 NMC|graphite pouch bag cells for three optimized electrolyte mixtures and the reference. The cells are cycled at 0.2 C continuously between 3 and 4.2 V vs. Li/Li^+

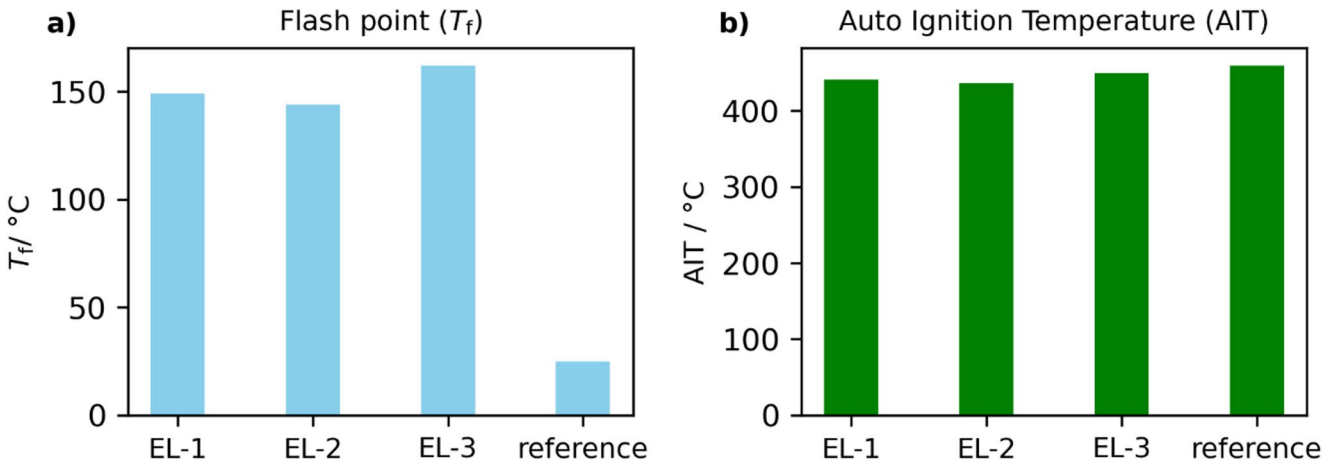

Fig. 13 Flash point (**a**) and auto ignition temperature (**b**) measurements from the three optimized electrolytes including the reference electrolyte. The reference refers to the sample EC + DMC + $LiPF_6$ electrolyte

here, with potential effects outlined. Determining the precise cause of $LiBF_4$ failure would require an investigation beyond the scope of this screening study. Nevertheless, these results clearly demonstrate that changes in cell format are nontrivial and can introduce significant challenges. This emphasizes the importance of verifying material performance at the system level, as even seemingly excellent materials may yield unexpected negative outcomes.

The other two electrolytes, EL-1 and EL-3, have a similar characteristic to the standard electrolyte in terms of both discharge capacity and aging. This demonstrates that the preselection process was successful, at least for the LiTFSI- and LiDFOB-containing electrolytes, and that it was possible to find an electrolyte mixture that can compete with commercial electrolytes during moderate discharge rates in terms of aging and cell performance. During the selection process, it can be observed clearly that electrolyte systems might be excluded too early due to excessive requirements for individual measurements (exclusion criteria) (e.g., if the density limit had been set slightly lower), which then leads to balanced electrolyte systems being rejected too early. Additionally, the order in which experiments are conducted can influence the selection process.

3.5 Thermal stability: flash point and auto-ignition temperature

Thermal stability was a critical requirement for the development of high-boiling, safe base electrolytes. Flash point (Fig. 13a) and auto ignition point (Fig. 13b) measurements are therefore necessary for a practical evaluation of potential hazardous situations. Compared to the conventional flame-exposure method for electrolytes [4], these values provide improved reliability and may serve as a basis for a more robust and reliable safety-characteristics profile [50, 51].

In comparison with the LP30 electrolyte, which ignites at 25 °C when exposed to a flame source, the novel electrolytes exhibit impressively high flash points above 140 °C. The flash point (T_f) of the electrolyte formulation is generally influenced by the components with the lowest flash point or with the predominant content [26, 49]. The high-boiling electrolyte mixtures therefore have excellent fire resistance. It is remarkable that the ignition points of LP30 and the new electrolytes did not differ much from each other, but were all around 450 °C. If a cell undergoes thermal runaway, the temperature can easily reach several hundred degrees [52].

This shows that despite the high flash points, which reflect ignition in the presence of an existing ignition source, the self-ignition of the electrolytes is similar, so that the relative safety of the electrolytes in an actual cell system should be investigated. TGA measurements (not shown here, preliminary data) confirm the behavior described, observing that the initial mass loss is highest at LP30. This can be attributed to the rapid volatilization of DMC. In addition, the salt $LiPF_6$ begins to decompose into LiF and PF_5 at temperatures below 100 °C [27]. In contrast, the EL-1/2/3 electrolytes show no significant mass loss up to about 100 °C.

4 Conclusion

Within the scope of the study, a screening for safe electrolytes was carried out. Several conclusions can be summarized that were obtained as results from the study:

(1) The question regarding the solubility of conductive salts, including the temperature ranges in which the mixture is liquid, is a practical starting method to significantly reduce the number of material combinations, i.e. to reduce the complexity of electrolyte screening.
(2) Conductivity and viscosity are often considered together. It was found that although high viscosity values tend to be associated with low conductivity, conductivity can vary considerably despite similar viscosity and must therefore be taken into account. In contrast, temperature-dependent measurements (conductivity, viscosity) did not result in any material narrowing, so that in a first step of the selection process, at least for chemically similar compounds, the very time-consuming temperature-dependent measurements can be avoided.
(3) The significance of the oxidative behavior is questionable due to the different materials in the preliminary test and cell, and led to only a few exclusions in material combinations.
(4) Half-cell measurements against lithium (or other alkali metals) enable screening that is largely free of additives.
(5) Full-cell coin cell tests provide a material-relevant basis for selection, where Coulomb efficiency analysis helps identify suitable mixtures. These tests may require additional additives to enable compatibility with specific electrode materials (e.g., certain carbonates with graphite).
(6) Preliminary coin cell results cannot be directly transferred to pouch-bag cells. For example, the $LiBF_4$-based electrolyte, despite promising coin cell performance, showed drastically lower capacity and faster aging in pouch cells. While the precise mechanisms were not clarified in this study, this underscores the importance of testing materials in the final target battery format.
(7) The popular flame tests, in which a flame is used to classify a compound (which then does not burn) as safe (corresponds to flash point measurement), raise doubts about the safety of electrolytes in the event of thermal runaway at significantly higher temperatures. Here, it was shown that the self-ignition temperature for all selected electrolytes is in a similar range, meaning that even electrolytes that initially exhibit "safe" behavior may burn.

The study therefore provides direct links to electrolytes that have proven promising in cell tests in terms of delayed flammability. On the other hand, it aims to provide guidance for the increasingly automated search for optimized electrolytes or mixtures, in some cases already with the help of AI methods, which tests make a meaningful contribution to narrowing down material combinations. Thirdly, it provides an experimental basis of various electrolyte characteristics for modelling and electrolyte calculation.

Supplementary Information The online version contains supplementary material available at https://doi.org/10.1007/s10800-026-02492-5.

Acknowledgements We would like to thank Sophie Dupont for carrying out individual measurements.

Author contributions All authors contributed to the study conception and design. Material preparation, data collection and analysis were performed by Zhengqi Wang and Andreas Hofmann. The first draft of the manuscript was written by Andreas Hofmann and all authors commented on previous versions of the manuscript. All authors read and approved the final manuscript.

Funding Open Access funding enabled and organized by Projekt DEAL.

Data availability Raw data can be found at Zenodo under https://doi.org/10.5281/zenodo.17303446.

Declarations

Competing interests The authors have no competing interests to declare that are relevant to the content of this article.

References

1. Liu Q, Zhao X, Yang Q, Hou L, Mu D, Tan G, Li L, Chen R, Wu F (2023) The progress in the electrolytes for solid state sodium-ion battery. Adv Mater Technol. https://doi.org/10.1002/admt.202200822
2. Piglowska M, Kurc B, Galinski M, Fuc P, Kaminska M, Szymlet N, Daszkiewicz P (2021) Challenges for safe electrolytes applied in lithium-ion cells-a review. Materials. https://doi.org/10.3390/ma14226783
3. Cui Y, Wan J, Ye Y, Liu K, Chou L, Cui Y (2020) A fireproof, lightweight, polymer-polymer solid-state electrolyte for safe lithium batteries. Nano Lett. https://doi.org/10.1021/acs.nanolett.9b04815
4. Du Y, Liu X, Chen L, Yin S, Xie Y-h, Li A, Liang X, Luo Y, Wu F, Mei Y, Xie D (2023) 3D hierarchical fireproof gel polymer electrolyte towards high-performance and comprehensive safety lithium-ion batteries. Chem Eng J. https://doi.org/10.1016/j.cej.2023.146605
5. Otsuki M, Ogino T, Amine K (2006) Investigation for flame-retardant additives for safety usage of lithium ion batteries. ECS Trans 2006:13–19
6. Mandal BK, Padhi AK, Shi Z, Chakraborty S, Filler R (2006) Thermal runaway inhibitors for lithium battery electrolytes. J Power Sources 161(2):1341–1345. https://doi.org/10.1016/j.jpowsour.2006.06.008
7. Hyung YE, Vissers DR, Amine K (2003) Flame-retardant additives for lithium-ion batteries. J Power Sources 119–121:383–387. https://doi.org/10.1016/S0378-7753(03)00225-8
8. Ouyang D, Guan J, Wan X, Liu B, Miao C, Wang Z (2024) Non-flammable all-fluorinated electrolyte enabling high-voltage and high-safety lithium-ion cells. ACS Appl Mater Interfaces. https://doi.org/10.1021/acsami.4c07886
9. An K, Tran YHT, Kwak S, Han J, Song SW (2021) Design of fire-resistant liquid electrolyte formulation for safe and long-cycled lithium-ion batteries. Adv Funct Mater. https://doi.org/10.1002/adfm.202106102
10. Noor Azleen MH, Ting P-M, Chen Z, Li Y, Shi Y, Akhavan S, Anouti M, Nikiforidis G (2025) A nonflammable deep eutectic electrolyte for safe and high-performance Lithium Iron Phosphate-Lithium Titanium Oxide cells. ACS Appl Energy Mater 8(14):10497–10507. https://doi.org/10.1021/acsaem.5c01337
11. Boisset A, Jacquemin J, Anouti M (2013) Physical properties of a new deep eutectic solvent based on lithium bis[(trifluoromethyl) sulfonyl]imide and N-methylacetamide as superionic suitable electrolyte for lithium ion batteries and electric double layer capacitors. Electrochim Acta 102:120–126. https://doi.org/10.1016/j.electacta.2013.03.150
12. Rauber D, Hofmann A, Philippi F, Kay CWM, Zinkevich T, Hanemann T, Hempelmann R (2021) Structure-property relation of trimethyl ammonium ionic liquids for battery applications. Appl Sci. https://doi.org/10.3390/app11125679
13. Chaudhari S, Nandi P, Subramaniam C (2025) Challenges, opportunities, and roadmap for ionic liquid-based electrolytes in advancing energy storage devices. Nanoscale 17(21):13121–13144. https://doi.org/10.1039/d5nr00522a
14. Shivani, Thakur RC, Thakur A, Sharma A, Sharma R (2025) Unravelling the prospects of electrolytes containing ionic liquids and deep eutectic solvents for next generation lithium batteries. J Energy Chem 105:482–500. https://doi.org/10.1016/j.jechem.2025.01.060
15. Balducci A (2017) Ionic liquids in lithium-ion batteries. Top Curr Chem 375(2):20. https://doi.org/10.1007/s41061-017-0109-8
16. Yao XL, Xie S, Chen CH, Wang QS, Sun JH, Li YL, Lu SX (2005) Comparative study of trimethyl phosphite and trimethyl phosphate as electrolyte additives in lithium ion batteries. J Power Sources 144(1):170–175. https://doi.org/10.1016/j.jpowsour.2004.11.042
17. Ouyang D, Wang K-H, Guan J, Wang Z (2024) Liquid non-aqueous electrolytes for high-voltage and high-safety Lithium-ion cells: a review. J Power Sources. https://doi.org/10.1016/j.jpowsour.2024.234550
18. Willstrand O, Quant M, Hynynen J (2025) Contaminations from lithium-ion battery fires—per- and polyfluoroalkyl substances (PFAS) in soot. Fire Technol 61(5):2889–2899. https://doi.org/10.1007/s10694-025-01708-y
19. Tawalbeh T, Rangarajan S, Liu H, Wang Y (2025) Fluorinated substances in Lithium-ion batteries and solid state batteries: recycling challenges and environmental impacts. J Power Sources. https://doi.org/10.1016/j.jpowsour.2025.237635
20. Li R, Zhao W, Li R, Gan C, Chen L, Wang Z, Yang X (2025) Leveraging machine learning for accelerated materials innovation in lithium-ion battery: a review. J Energy Chem 106:44–62. https://doi.org/10.1016/j.jechem.2025.02.038
21. Matsuda S, Takahashi M (2025) Multichannel electrochemical cell and liquid-handling dispenser for high-throughput combinatorial screening of multicomponent electrolytes for advanced Lithium-ion batteries. Batter Supercaps. https://doi.org/10.1002/batt.202400777
22. Bolloju S, Vangapally N, Elias Y, Luski S, Wu N-L, Aurbach D (2025) Electrolyte additives for Li-ion batteries: classification by elements. Prog Mater Sci. https://doi.org/10.1016/j.pmatsci.2024.101349
23. Brijesh K, Jareer M, Sagar GL, Mukesh P, Amudha A, Mandal D, Nagaraja HS, Shahgaldi S (2025) Advanced electrolyte additives for lithium-ion batteries: classification, function, and future directions. J Phys Chem C. https://doi.org/10.1021/acs.jpcc.5c01331
24. Hofmann A, Merklein L, Schulz M, Hanemann T (2014) Anodic aluminum dissolution of LiTFSA containing electrolytes for Li-Ion-batteries. Electrochim Acta 116:388–395. https://doi.org/10.1016/j.electacta.2013.11.085
25. Hofmann A, Schulz M, Winkler V, Hanemann T (2014) Anodic aluminum dissolution in conducting salt containing electrolytes for lithium-ion batteries. J Electrochem Soc 161(3):A431–A438. https://doi.org/10.1149/2.094403jes
26. Hess S, Wohlfahrt-Mehrens M, Wachtler M (2015) Flammability of Li-Ion battery electrolytes: flash point and self-extinguishing time measurements. J Electrochem Soc 162(2):A3084–A3097. https://doi.org/10.1149/2.0121502jes
27. Campion CL, Li W, Lucht BL (2005) Thermal decomposition of LiPF6-based electrolytes for Lithium-ion batteries. J Electrochem Soc 152(12):A2327. https://doi.org/10.1149/1.2083267
28. Zhou F, Liu L, Hou X, Zhang Q, Guo S, Huang B, Li J, Wang C, Li P (2025) Synergistic effect of vinylene carbonate and fluoroethylene carbonate in constructing a robust yet flexible SEI for high performance black Phosphorus anodes. J Alloys Compd. https://doi.org/10.1016/j.jallcom.2025.181804
29. Wang Q, He X, Fan X, Ma Y, Su Y, Zhang D, Li Z, Sun H, Sun Q, Wang B, Fan LZ (2024) Enhancing stable LiF-rich interface formation of polyester based electrolyte using fluoroethylene carbonate for quasi-solid state lithium metal batteries. Int J Hydrogen Energy 67:608–617. https://doi.org/10.1016/j.ijhydene.2024.04.154
30. Wuamprakhon P, Songthan R, Sangsanit T, Santiyuk K, Phojaroen J, Homlamai K, Tejangkura W, Sawangphruk M (2024) Designing electrolytes for enhancing stability and performance

of Lithium-ion capacitors at large-scale cylindrical cells. J Power Sources. https://doi.org/10.1016/j.jpowsour.2024.235331
31. Qin G, Zhang J, Chen H, Li H, Hu J, Chen Q, Hou G, Tang Y (2024) Lithium difluoro(oxalate)borate as electrolyte additive to form uniform, stable and LiF-rich solid electrolyte interphase for high performance Lithium ion batteries. Surf Interfaces. https://doi.org/10.1016/j.surfin.2024.104297
32. Hofmann A, Hanemann T (2015) Novel electrolyte mixtures based on dimethyl sulfone, ethylene carbonate and LiPF6 for lithium-ion batteries. J Power Sources 298:322–330. https://doi.org/10.1016/j.jpowsour.2015.08.071
33. McOwen DW, Seo DM, Borodin O, Vatamanu J, Boyle PD, Henderson WA (2014) Concentrated electrolytes: decrypting electrolyte properties and reassessing Al corrosion mechanisms. Energy Environ Sci 7(1):416–426. https://doi.org/10.1039/c3ee42351d
34. Hofmann A, Werth F, Ho weling A, Hanemann T (2015) Investigation of the oxidative stability of Li-Ion battery electrolytes using cathode materials. ECS Electrochem Lett 4(12):A141–A144. https://doi.org/10.1149/2.0071512eel
35. Zhang XQ, Cheng XB, Chen X, Yan C, Zhang Q (2017) Fluoroethylene carbonate additives to render uniform Li deposits in lithium metal batteries. Adv Funct Mater. https://doi.org/10.1002/adfm.201605989
36. Markevich E, Salitra G, Chesneau F, Schmidt M, Aurbach D (2017) Very stable Lithium metal stripping–plating at a high rate and high areal capacity in fluoroethylene carbonate-based organic electrolyte solution. ACS Energy Lett 2(6):1321–1326. https://doi.org/10.1021/acsenergylett.7b00300
37. Smith A, Stüble P, Leuthner L, Hofmann A, Jeschull F, Mereacre L (2023) Potential and limitations of research battery cell types for electrochemical data acquisition. Batteries Supercaps. https://doi.org/10.1002/batt.202300080
38. Besenhard JO, Winter M, Yang J, Biberacher W (1995) Filming mechanism of lithium-carbon anodes in organic and inorganic electrolytes. J Power Sources 54(2):228–231. https://doi.org/10.1016/0378-7753(94)02073-C
39. Ota H, Sakata Y, Inoue A, Yamaguchi S (2004) Analysis of Vinylene Carbonate derived SEI layers on Graphite anode. J Electrochem Soc 151:A1659. https://doi.org/10.1149/1.1785795
40. Aurbach D, Gamolsky K, Markovsky B, Gofer Y, Schmidt M, Heider U (2002) On the use of vinylene carbonate (VC) as an additive to electrolyte solutions for Li-ion batteries. Electrochim Acta 47(9):1423–1439. https://doi.org/10.1016/S0013-4686(01)00858-1
41. Stockhausen R, Hofmann A, Gehrlein L, Bergfeldt T, Müller M, Ehrenberg H, Smith A (2021) Quantifying absolute amounts of electrolyte components in lithium-ion cells using HPLC. J Electrochem Soc. https://doi.org/10.1149/1945-7111/ac1894
42. Pan Y, Wang G, Lucht BL (2016) Cycling performance and surface analysis of Lithium bis(trifluoromethanesulfonyl)imide in propylene carbonate with graphite. Electrochim Acta 217:269–273. https://doi.org/10.1016/j.electacta.2016.09.080
43. Zhao X, Zhuang Q-C, Xu S-D, Xu Y-X, Shi Y-L, Zhang X-X (2015) A new insight into the content effect of Fluoroethylene Carbonate as a film forming additive for Lithium-Ion batteries. Int J Electrochem Sci 10(3):2515–2534. https://doi.org/10.1016/s1452-3981(23)04865-4
44. Markevich E, Salitra G, Aurbach D (2017) Fluoroethylene carbonate as an important component for the formation of an effective solid electrolyte interphase on anodes and cathodes for advanced Li-ion batteries. ACS Energy Lett 2(6):1337–1345. https://doi.org/10.1021/acsenergylett.7b00163
45. Webber A (1991) Conductivity and viscosity of solutions of $LiCF_3SO_3$, $Li(CF_3SO_2)_2N$, and their mixtures. J Electrochem Soc 138(9):2586. https://doi.org/10.1149/1.2087287
46. Michan AL, Parimalam BS, Leskes M, Kerber RN, Yoon T, Grey CP, Lucht BL (2016) Fluoroethylene carbonate and vinylene carbonate reduction: understanding lithium-ion battery electrolyte additives and solid electrolyte interphase formation. Chem Mater 28(22):8149–8159. https://doi.org/10.1021/acs.chemmater.6b02282
47. Wang A, Kadam S, Li H, Shi S, Qi Y (2018) Review on modeling of the anode solid electrolyte interphase (SEI) for lithium-ion batteries. npj Comput Mater. https://doi.org/10.1038/s41524-018-0064-0
48. Tasaki K (2005) Solvent decompositions and physical properties of decomposition compounds in Li-ion battery electrolytes studied by DFT calculations and molecular dynamics simulations. J Phys Chem B 109(7):2920–2933. https://doi.org/10.1021/jp047240b
49. Xu K (2004) Nonaqueous liquid electrolytes for lithium-based rechargeable batteries. Chem Rev 104(10):4303–4418. https://doi.org/10.1021/cr030203g
50. Guo F, Hase W, Ozaki Y, Konno Y, Inatsuki M, Nishimura K, Hashimoto N, Fujita O (2019) Experimental study on flammability limits of electrolyte solvents in lithium-ion batteries using a wick combustion method. Exp Therm Fluid Sci. https://doi.org/10.1016/j.expthermflusci.2019.109858
51. Huang XH, Chung YH, Guo GS, Shu CM (2025) Investigating the thermal stability and explosion characteristics of electrolytes composed of different ratios of carbonate organic solvents. J Loss Prev Process Ind. https://doi.org/10.1016/j.jlp.2024.105509
52. Jhu C-Y, Wang Y-W, Wen C-Y, Shu C-M (2012) Thermal runaway potential of $LiCoO_2$ and $Li(Ni_{1/3}Co_{1/3}Mn_{1/3})O_2$ batteries determined with adiabatic calorimetry methodology. Appl Energy 100:127–131. https://doi.org/10.1016/j.apenergy.2012.05.064